E-ARTICLE

Physical Determinants of Phytoplankton Production, Algal Stoichiometry, and Vertical Nutrient Fluxes

Christoph G. Jäger,[1,2,*] Sebastian Diehl,[1,†] and Maximilian Emans[3]

1. Department Biologie II, Ludwig-Maximilians-Universität München, Grosshaderner Strasse 2, 82152 Planegg-Martinsried, Germany; 2. Department of Ecology and Environmental Science, Umeå University, 90187 Umeå, Sweden; 3. AVL List GmbH, Hans-List-Platz 1, 8020 Graz, Austria

Submitted April 8, 2009; Accepted September 22, 2009; Electronically published February 23, 2010

Enhancement: appendix.

ABSTRACT: Most phytoplankters face opposing vertical gradients in light versus nutrient supplies but have limited capacities for vertical habitat choice. We therefore explored a dynamical model of negatively buoyant algae inhabiting a one-dimensional water column to ask how water column depth and turbulence constrain total (areal) phytoplankton biomass. We show that the population persistence boundaries in water column depth–turbulence space are set by sinking losses and light limitation but that nutrients are most limiting to total biomass in water columns that are neither too shallow or too weakly mixed (where sinking losses prevail) nor too deep and turbulent (where light limitation prevails). In shallow waters, the most strongly limiting process is nutrient influx to the bottom of the water column (e.g., from sediments). In deep waters, the most strongly limiting process is turbulent upward transport of nutrients to the photic zone. Consequently, the highest total biomasses are attained in turbulent waters at intermediate water column depths and in deep waters at intermediate turbulences. These patterns are insensitive to the assumption of fixed versus flexible algal carbon-to-nutrient stoichiometry, and they arise irrespective of whether the water column is a surface layer above a deep water compartment or has direct contact with sediments.

Keywords: carbon-to-phosphorus ratio, light, mixing intensity, nutrients, spatial heterogeneity, water column depth.

Introduction

Primary production depends critically on the supply of two fundamentally different types of resources, that is, light and mineral nutrients. While photosynthetically active radiation is always supplied externally and a photon can only be used once for photosynthesis, sustained nutrient supply requires efficient storage and recycling of nutrients within the ecosystem. In most pelagic aquatic habitats, planktonic primary producers therefore face a critical environmental trade-off, that is, a spatial separation of the zones where nutrients are recycled and the zones where they are needed for primary production. Because light is vertically attenuated by water molecules and dissolved and suspended materials, primary production is restricted to an upper surface layer, the euphotic zone (Kirk 1994). Most living algal cells and essentially all detrital material have, however, a higher specific density than that of water (Smayda 1969; Reynolds 1984). Consequently, in sufficiently deep bodies of water, both living algae and detritus tend to sink out of the euphotic zone, and a fraction of their nutrient content is eventually mineralized in deep water layers or in the sediment (Wetzel 1983; Antia 2005; Peterson et al. 2005). Turbulent mixing is then required to transport recycled nutrients back into the euphotic zone. Thus, physical characteristics of the water column—most notably, its depth and the degree of turbulent mixing—are key factors influencing the spatial separation of the nutrient recycling zones, the nutrient use by primary producers, and the vertical transport between the zones (Klausmeier and Litchman 2001; Diehl 2002; Huisman et al. 2006).

That water column depth and mixing intensity are crucial determinants of phytoplankton production has been known for a long time (Riley et al. 1949; Sverdrup 1953). Recently, however, this topic has received renewed interest. All else being equal, an increase in water column depth decreases specific sedimentation losses, but it also decreases depth-averaged light availability (Visser et al. 1996; Huisman 1999; Diehl et al. 2002; Ptacnik et al. 2003). Similarly, enhanced turbulence reduces sedimentation losses but increases downward mixing of algae to more light-limited depths (Condie and Bormans 1997; Huisman et al. 1999; O'Brien et al. 2003). Consequently, phytoplankton population growth can be strongly limited by sinking losses in shallow, weakly mixed water columns and by light in deep, turbulent water columns. To maintain a population of sinking algae therefore requires a minimal

* Corresponding author; e-mail: christoph.jager@emg.umu.se.

† Present address: Department of Ecology and Environmental Science, Umeå University, 90187 Umeå, Sweden.

Am. Nat. 2010. Vol. 175, pp. E91–E104.
DOI: 10.1086/650728

water column depth and a minimal turbulence to counteract sinking losses (Diehl 2002; Huisman and Sommeijer 2002). Conversely, the maintenance of populations of both sinking and buoyant algae requires that the water column does not exceed a maximal depth and that mixing intensity remain below a threshold of maximal turbulence to counteract entrainment below the euphotic depth (Sverdrup 1953; Huisman et al. 1999, 2002; Peeters et al. 2007).

While the influences of water column depth and turbulence on the limitation of algal production by sinking versus vertical light attenuation are fairly well understood in theory, a similarly comprehensive understanding of their influences on nutrient limitation of algal production is still lacking. So far, the influence of water column depth on nutrient dynamics has been theoretically explored primarily for well-mixed systems. In such systems, phytoplankton production again tends to be limited by sinking losses in shallow water columns and by low average light levels in deep water columns, whereas at intermediate water column depths, algal production is limited by nutrient availability (Huisman and Weissing 1995; Diehl 2002; Diehl et al. 2005; Berger et al. 2006). It seems most plausible to expect that reduced turbulence may alter this pattern by changing vertical nutrient fluxes, but this important aspect remains largely unexplored (but see Huisman et al. 2006).

Pelagic algal and nutrient dynamics may be further complicated by variability in the elemental composition of phytoplankton in response to the relative supplies of light and nutrients, as influenced by, for example, water column depth or vertical position in the water column (Sterner et al. 1997; Bertilsson et al. 2003; Berger et al. 2006). Algal stoichiometry, in turn, feeds back on the nutrient dependence of algal growth rates, the amount of algal self-shading produced per unit of assimilated nutrient, and the nutrient fluxes associated with algal sinking (Rothhaupt 1991; Elser and George 1993; Geider et al. 1998; Park et al. 2004; Christian 2005; Diehl et al. 2005). Clearly, a comprehensive analysis of the influences of water column depth and turbulence on phytoplankton dynamics must consider nutrient dynamics and algal nutrient limitation, and it should also include flexible algal nutrient-to-carbon stoichiometry.

We performed such a comprehensive analysis with a model describing the temporal and spatial dynamics of light, nutrients, and a population of negatively buoyant algae with flexible nutrient-to-carbon stoichiometry in a one-dimensional water column. We show that the persistence boundaries of the algal population in water column depth–turbulence space are set by sinking losses and light limitation but that nutrient supply is the primary limiting factor for algal biomass in water columns that are neither too shallow or too weakly mixed (where sinking losses prevail) nor too deep and turbulent (where light limitation prevails). We also show that the nutrient influx to the bottom of the water column (e.g., from sediments) becomes most limiting to biomass in well-mixed water columns, whereas turbulent upward transport of nutrients becomes most limiting in weakly mixed water columns. Consequently, the highest depth-integrated biomasses are attained in deep water at intermediate turbulence, where neither sinking nor light attenuation nor nutrient availability is particularly limiting. Numerical analyses confirm that these patterns are insensitive to the assumption of fixed versus flexible algal carbon-to-nutrient stoichiometry, and they apply both to water columns in direct contact with the sediment and to surface layers of deeper, stratified water columns.

The Model

Basic Model Structure and Boundary Fluxes

The basic model (hereafter called the standard model) consists of a one-dimensional water column and a sediment layer. We assume that algal production is limited by supplies of light and a single mineral nutrient and that the system is closed for nutrients. A system of three partial differential equations, one ordinary differential equation, and one algebraic equation describes the dynamics of the concentrations of algal carbon biomass (A), particulate nutrients bound in algae (R_b), and dissolved mineral nutrients (R_d) in the water column; of light intensity (I) in the water column; and of the pool of sedimented nutrients (R_s):

$$\frac{\partial A}{\partial t} = p(I, q)A - l_{bg}A - v\frac{\partial A}{\partial z} + d\frac{\partial^2 A}{\partial z^2}, \quad (1)$$

$$\frac{\partial R_b}{\partial t} = \rho(q, R_d)A - l_{bg}R_b - v\frac{\partial R_b}{\partial z} + d\frac{\partial^2 R_b}{\partial z^2}, \quad (2)$$

$$\frac{\partial R_d}{\partial t} = l_{bg}R_b - \rho(q, R_d)A + d\frac{\partial^2 R_d}{\partial z^2}, \quad (3)$$

$$I(z) = I_0 \exp -\left(\int_0^z kA dz + k_{bg}z\right), \quad (4)$$

$$\frac{dR_s}{dt} = vR_b(z_{max}) - rR_s. \quad (5)$$

In all of the numerical simulations, the limiting nutrient was assumed to be phosphorus. All state variables and parameters are defined with units in table 1. The water column runs from depth 0 at the surface to z_{max} at the bottom. Mixing of water, suspended algae, and dissolved nutrients are described by the turbulent-diffusion coefficient d, which is assumed to be constant over depth z. Phytoplankton sink through the water column with ve-

Table 1: Definitions and units of parameters and variables and basic set of parameter values and initial conditions

Parameter/ variable	Value	Definition (units)
a	.1	Exchange rate between surface and deep water layers in the open model (day^{-1})
d	.01–1,000[a]	Turbulent-diffusion coefficient ($m^2\ day^{-1}$)
h	120	Half-saturation constant of light-dependent algal production (μmol photons $m^{-2}\ s^{-1}$)
I_0	300	Light intensity at the surface (μmol photons $m^{-2}\ s^{-1}$)
k	.0003	Specific light-attenuation coefficient of algal biomass ($m^2\ mg\ C^{-1}$)
k_{bg}	.2, .4, .8[a]	Background light-attenuation coefficient (m^{-1})
l_{bg}	.1	Specific algal maintenance respiration losses (day^{-1})
m	1.5	Half-saturation constant of algal nutrient uptake (mg P m^{-3})
μ'_{max}	1.08	Maximum specific algal production rate in the fixed-stoichiometry and light-limitation models (day^{-1})
μ_{max}	1.2	Maximum specific algal production rate in all models except the fixed-stoichiometry and light-limitation models (day^{-1})
q_{fix}	.0244	Algal nutrient quota in the fixed-stoichiometry model (mg P mg C^{-1})
q_{max}	.04	Maximum algal nutrient quota (mg P mg C^{-1})
q_{min}	.004	Minimum algal nutrient quota (mg P mg C^{-1})
r	.02, 1[b]	Specific mineralization rate of sedimented nutrients (day^{-1})
ρ_{max}	.2	Maximum specific algal nutrient uptake rate (mg P mg $C^{-1}\ day^{-1}$)
R_h	30	Concentration of dissolved nutrients in the deep water layer in the open model (mg P m^{-3})
v	0, .25, .5[a]	Algal sinking velocity ($m\ day^{-1}$)
z_{max}	1–50[a]	Depth of water column (m)
A	100[c]	Algal carbon density (mg C m^{-3})
I		Light intensity (μmol photons $m^{-2}\ s^{-1}$)
p		Specific algal production rate (day^{-1})
q		Algal nutrient quota (mg P mg C^{-1})
R_b	2.2[c]	Concentration of particulate nutrients bound in algae (mg P m^{-3})
R_d	10, 30[a,c]	Concentration of dissolved nutrients (mg P m^{-3})
R_s	0[c]	Pool of sedimented nutrients (mg P m^{-2})
ρ		Specific algal nutrient uptake rate (mg P mg $C^{-1}\ day^{-1}$)
W		Depth-integrated algal biomass (mg C m^{-2})
z		Depth below water surface (m)

[a] Range of environmental conditions examined.
[b] Instant-mineralization model.
[c] Initial values.

locity v and have constant specific maintenance losses l_{bg}. Specific algal growth rate p is an increasing, saturating function of light intensity I and algal nutrient quota q (nutrient content per carbon biomass):

$$p(I, q) = \mu_{max}\left(1 - \frac{q_{min}}{q}\right)\frac{I}{h + I}, \tag{6}$$

where μ_{max} is the nominal maximum specific production rate (theoretically attained when $q \to \infty$), q_{min} is the algal nutrient quota at which growth ceases, and h is the half-saturation constant of light-dependent production. The multiplicative form of light and nutrient limitation of algal production is computationally convenient but also empirically justified (Senft 1978). We assume that the vertical light gradient follows Lambert-Beer's law. Light intensity at depth z then depends on surface light intensity I_0 and on the integral of light attenuation by algal biomass (with specific attenuation coefficient k) and nonalgal components k_{bg} above depth z (eq. [4]).

Algal nutrient quota q is calculated as

$$q = \frac{R_b}{A}. \tag{7}$$

This calculation of q is correct as long as identical coefficients for sinking and diffusion are used in equations (1) and (2). The procedure makes the implicit assumption that all algae at a given depth have the average cell quota of that depth, and thus it ignores the fact that sinking and turbulence blend algae from depth strata differing in q. Because p increases nonlinearly with q, the use of average q in equation (6) slightly overestimates the true production rate. The error introduced by this procedure, however, is negligible because algae from neighboring depth strata have similar cell quotas and quickly adapt them to local light-nutrient conditions.

Algae take up dissolved nutrients and transform them into particulate nutrients at the rate

$$\rho(q, R_d) = \rho_{max}\left(1 - \frac{q - q_{min}}{q_{max} - q_{min}}\right)\frac{R_d}{m + R_d}, \quad (8)$$

where ρ_{max} is the maximum specific uptake rate, m is the half-saturation constant of nutrient uptake, and q_{max} is the algal nutrient quota at which uptake ceases. At a given dissolved-nutrient concentration, nutrient uptake is thus a linear function of q, with no uptake at q_{max} and maximum uptake at q_{min}. We assume that algae excrete mineral nutrients and respire carbon at the same specific rate l_{bg}. At the other extreme, one could assume that maintenance involves only carbon respiration but no nutrient losses (Diehl et al. 2005). Because excreted nutrients are almost instantly taken up by the algae excreting them (except when q is close to q_{max}), results are not sensitive to this assumption.

The boundary conditions are set such that algal biomass and particulate nutrients neither leave nor enter the system at the surface (no flux at $z = 0$) but sink out at the bottom of the water column (convective flux at $z = z_{max}$). The latter condition implies that the fluxes of particulate carbon and nutrients into the sediment are $-vA(z_{max})$ and $-vR_b(z_{max})$, respectively. Particulate nutrients are mineralized in the sediment and return to the water column in dissolved mineral form at rate r. Dissolved nutrients therefore have an influx of mineralized nutrients rR_s at the bottom of the water column and no-flux conditions at the surface. A table with the boundary conditions is given in the appendix (table A1). For computational convenience, we calculated the temporal dynamics of the vertical light gradient and sedimented nutrients not with equations (4) and (5) but instead with the equivalent formulations shown in the appendix (the technical details of our numerical approach are also described there).

Model Analyses

We performed extensive numerical simulations to explore how water column depth, turbulence, and other environmental factors influence the dynamics of our model system. All parameter values not varied among simulations are representative of a generic temperate lake inhabited by phytoplankton with average traits (e.g., see Andersen 1997, chap. 3.5) that are very similar or identical to the ones used in Diehl et al. (2005; table 1). Simulations were performed with COMSOL 3.2 with a vertical grid spacing of 0.02 m and an automatic time step, and they were run to equilibrium. Because nutrient limitation is the focus of our analyses, we explored seven variants of the model that differ with respect to the form of nutrient supply and the degree of nutrient limitation of phytoplankton production.

Standard Model. We first investigated how different levels of turbulence ($d = 0.01$–$1{,}000$ m^2 day^{-1}, spanning a range from fully stratified to fully mixed) cross-classified with 50 different water column depths (1–50 m, evenly spaced at 1-m intervals) affect equilibrium patterns of phytoplankton biomass, production and sedimentation, algal nutrient quota, and dissolved and sedimented nutrients in the standard model. These analyses were performed with a background light-attenuation coefficient $k_{bg} = 0.4$ m^{-1} (corresponding to a typical freshwater lake), an algal sinking velocity $v = 0.25$ m day^{-1}, a mineralization rate of sedimented nutrients $r = 0.02$ day^{-1}, and initially homogeneous vertical distributions of algal biomass and dissolved nutrients of 100 mg C m^{-3} and 30 mg P m^{-3}, respectively. The initial pool of sedimented nutrients was 0, and the initial concentration of particulate nutrients was 2.2 mg P m^{-3}, yielding an initial algal nutrient quota of 0.022 mg P mg C^{-1} (close to the Redfield ratio) and a total nutrient concentration ($R_d + R_b$) of 32.2 mg P m^{-3}. We verified the robustness of the observed patterns by running simulations at different levels of background turbidity and initial dissolved-nutrient concentration and by varying algal sinking velocity.

Fixed-Stoichiometry Model. To assess the extent to which the system's responses to physical water column characteristics are influenced by flexible algal nutrient-to-carbon stoichiometry, we repeated all analyses with a model variant in which the algal nutrient quota was fixed at the Redfield ratio ($q_{fix} = 0.0244$ mg P mg C^{-1}). In this fixed-stoichiometry model, specific algal production rate p in equation (1) depends on the external nutrient concentration R_d as

$$p(I, R_d) = \mu'_{max}\frac{R_d}{m + R_d}\frac{I}{h + I}, \quad (9)$$

and algal nutrient uptake rate is proportional to algal production rate. Equation (3) is therefore replaced by

$$\frac{\partial R_d}{\partial t} = q_{fix}l_{bg}A - q_{fix}p(I, R_d)A + d\frac{\partial^2 R_d}{\partial z^2}. \quad (10)$$

A separate equation for particulate nutrients is not necessary, because $R_b = q_{fix}A$. Boundary conditions, equations (4) and (5), and parameter values are identical to those in the standard model. The flux of nutrients into the sediment is now calculated by the flux of biomass A multiplied by q_{fix}.

While μ'_{max} in equation (9) is a true maximum specific growth rate, μ_{max} in the standard model is a nominal parameter, with the realizable maximum specific growth rate being $\mu_{max}(1 - q_{min}/q_{max})$. To make quantitative comparisons between the fixed-stoichiometry and standard mod-

els meaningful, we therefore set μ'_{max} in equation (9) to a fraction $(1 - q_{min}/q_{max})$ of μ_{max}. Note that the fixed-stoichiometry model is not a special case of the standard model. It is true that, at equilibrium, algal growth in the standard model is proportional to nutrient uptake and the growth and nutrient uptake terms (eqq. [6], [8]) can then be merged and replaced by equation (9) with an appropriately scaled μ'_{max}. However, the corresponding equilibrium algal nutrient quota, and hence the scaling of μ'_{max}, varies in space and with environmental conditions (fig. 1).

Light-Limitation, Mixed-Nutrient, and Instant-Mineralization Models. To assess which factors (sinking, light attenuation, overall nutrient supply, recycling of sedimented nutrients, or upward transport of recycled nutrients) limit phytoplankton biomass in the standard model most strongly under different combinations of water column depth and turbulence, we repeated all analyses under the assumptions of pure light limitation of algal production (light-limitation model), of an almost instant remineralization of sedimented nutrients (instant-mineralization model with a specific mineralization rate $r = 1$ day^{-1}), and that dissolved nutrients were always mixed with the maximal intensity $d = 1{,}000$ m^2 day^{-1} while phytoplankton biomass (and particulate nutrients) experienced a full range of turbulences, from 0.01 to 1,000 m^2 day^{-1} (mixed-nutrient model). In the mixed-nutrient model, the influences of turbulence on phytoplankton sinking and entrainment are uncoupled from influences of turbulence on nutrient transport. The speed with which sedimented nutrients are resupplied to the photic zone then depends solely on the mineralization rate in the sediment. In contrast, in the instant-mineralization model, nutrients

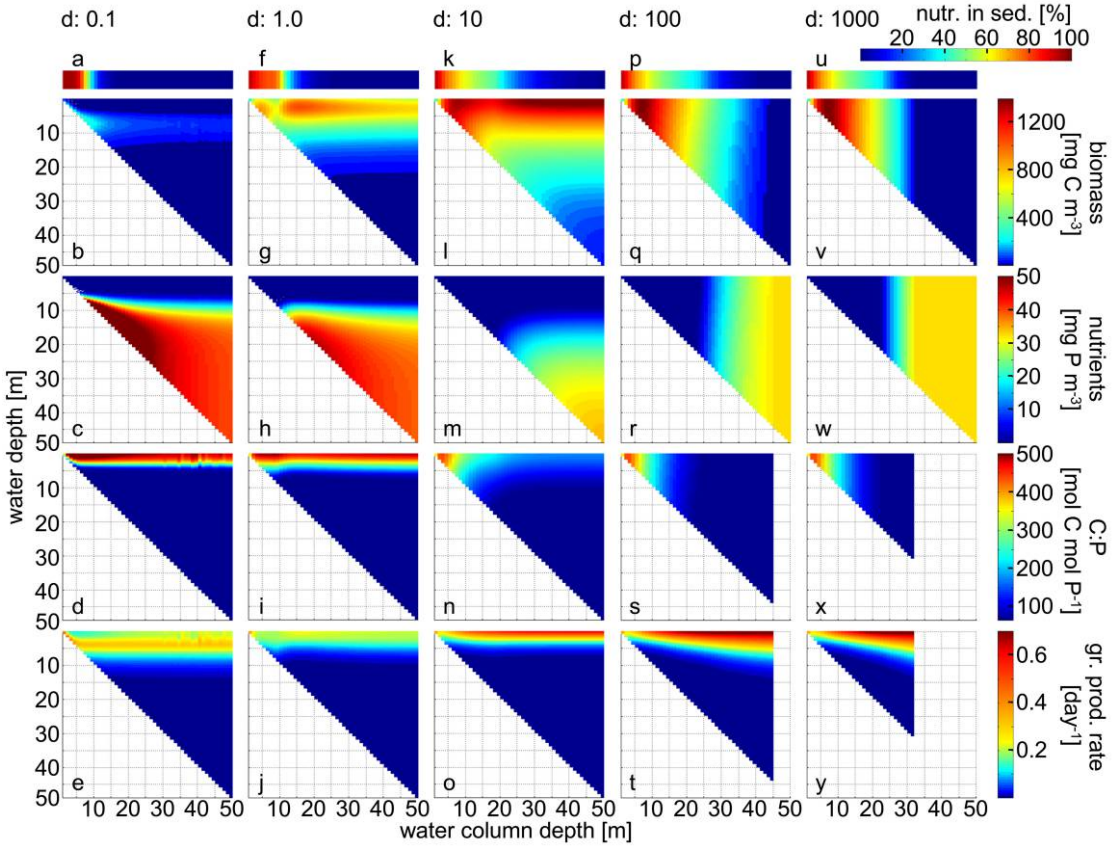

Figure 1: Standard model. Equilibrium vertical profiles (*Y*-axes) at different total water column depths (*X*-axes) of algal biomass concentration (*b*, *g*, *l*, *q*, *v*), dissolved-nutrient concentration (*c*, *h*, *m*, *r*, *w*), algal C : P ratio (*d*, *l*, *n*, *s*, *x*), and specific algal gross production rate (*e*, *j*, *o*, *t*, *y*), and the proportion of total nutrients stored in the sediment (*a*, *f*, *k*, *p*, *u*) at different water column depths. Columns show data for five different levels of turbulence (*d*, with values of 0.1, 1, 10, 100, and 1,000 m^2 day^{-1}). Color legends are on the right end of each row. Algae die out at total water column depths >45 and >32 m at $d = 100$ and 1,000 m^2 day^{-1}, respectively. Algal C : P ratios and gross production rates are therefore not shown for these water column depths. At $d = 0.1$ m^2 day^{-1}, the system shows persistent, small oscillations in deep water columns that blur the graphs of algal C : P ratio and gross production rate.

cannot accumulate in the sediment. The speed with which sedimented nutrients are resupplied to the photic zone then depends solely on the speed of turbulent upward transport. Finally, in the light-limitation model, phytoplankton is completely released from nutrient limitation. In the light-limitation model, specific algal production rate p in equation (1) is thus dependent only on light intensity I:

$$p(I) = \mu'_{\max}\frac{I}{h + I}. \quad (11)$$

As was already explained for the fixed-stoichiometry model, for the quantitative comparison of the light-limitation model with the standard and the mixed-nutrient models, the maximum specific production rate $\mu'_{\max}$ in equation (11) had to be set to $1 - q_{\min}/q_{\max}$ of $\mu_{\max}$. Equations for dissolved nutrients, particulate nutrients bound in algae, and the pool of sedimented nutrients are not necessary in the light-limitation model.

Areal-Nutrient Model. In the standard model, the total amount of nutrients in the system is proportional to the water column depth. We also explored the other extreme of the closed-system nutrient supply (called the areal-nutrient model) by assuming that the total amount of nutrients (per area) is independent of water column depth and is thus the same in all water columns. We implemented this assumption by setting initial dissolved-nutrient concentration equal to 1,500/(water column depth) mg P m^{-3}. Thus, all water columns in the areal-nutrient model received the same initial areal amount of dissolved nutrients as a 50-m-deep water column in the standard model.

Open Model. Finally, we relaxed the assumptions of a closed system and contact of the water column with the sediment. Instead, we assumed that a surface layer described by equations (1)–(4) was separated from the sediments by a phytoplankton-free deep-water layer with a constant nutrient concentration R_h. This open model mimics a water column consisting of a surface layer and a deep-water layer separated by a sharp thermocline. The fluxes of nutrients across this thermocline were calculated as $a(R_h - R_d)$, where the diffusive nutrient exchange rate a between the surface and deep water was implemented as a boundary condition at the bottom of the surface layer ($z_{\max}$). Parameter values are given in table 1. An equation for the pool of sedimented nutrients is not necessary in the open model.

Most systems came close to equilibrium within 30–200 days, with the exception of deep, well-mixed systems, where the extinction of algal populations required a longer time span. The time to truly reach equilibrium can, however, be quite long. We therefore first evaluated equilibrium states on day 10,000. For all simulation outputs, we then calculated equilibrium vertical distributions of the following state variables: algal biomass, dissolved nutrients, algal nutrient quota (presented as molar C : P ratio $= (1/q)(31/12)$), specific algal gross production rate ($p(I, q)$), and the pool of sedimented nutrients. From these, we derived the following quantities: algal standing stock per area W (depth-integrated algal biomass), depth-averaged dissolved-nutrient concentration, specific sedimentation rate (flux of biomass to the sediment/W), and the depth $z(A_{\max})$ at which the maximum concentration of algal biomass occurs within the water column. Finally, we derived a quantity called optimal mixing intensity (mixing intensity yielding the highest depth-integrated biomass W for a given water column depth $z_{\max}$) and compared its positions in z-d space for the standard, mixed-nutrient, and light-limitation models as well as its dependence on background turbidity and nutrient enrichment in the standard model.

Results

Effects of Water Column Depth and Turbulence in the Standard Model

At all levels of turbulence, a minimum water column depth of ~0.4 m (red line in fig. 3; not shown in figs. 1 and 2) is required to sustain an algal population, because sedimentation loss rate exceeds the maximum algal production rate in extremely shallow water columns. Similarly, at all water column depths, a minimum turbulence of ~0.03 m^2 day^{-1} (red line in fig. 3; not shown in figs. 1 and 2) is required to sustain an algal population, because the downward movement of sinking algae must be counteracted by turbulence.

At high turbulence ($d = 100$–$1{,}000$ m^2 day^{-1}), there are nearly no vertical gradients in algal biomass, dissolved nutrients, and algal C : P ratio (fig. 1*q*–1*s*, 1*v*–1*x*). The degree of algal nutrient limitation is therefore the same everywhere in the water column. Consequently, specific algal production is highest at the surface and decreases vertically in parallel with the light gradient (fig. 1*t*, 1*y*). In water columns <5 m high, sedimentation losses (fig. 2*d*) cause >75% of total nutrients to be locked up in the sediment (fig. 1*p*, 1*u*). The resupply of nutrients to the water column is then limited by the mineralization rate in the sediment. Consequently, the algal C : P ratio is high (fig. 1*s*, 1*x*) and production is nutrient limited. With increasing water column depth, specific sedimentation losses and the proportion of nutrients in the sediment decrease (figs. 1*p*, 1*u*, 2*d*). Algal nutrient limitation (C : P ratio) thus decreases, and specific algal production at a given depth in the water column increases over the entire gradient of increasing water column depths (fig. 1*s*, 1*t*, 1*x*, 1*y*). Initially, algal biomass therefore also increases with increasing

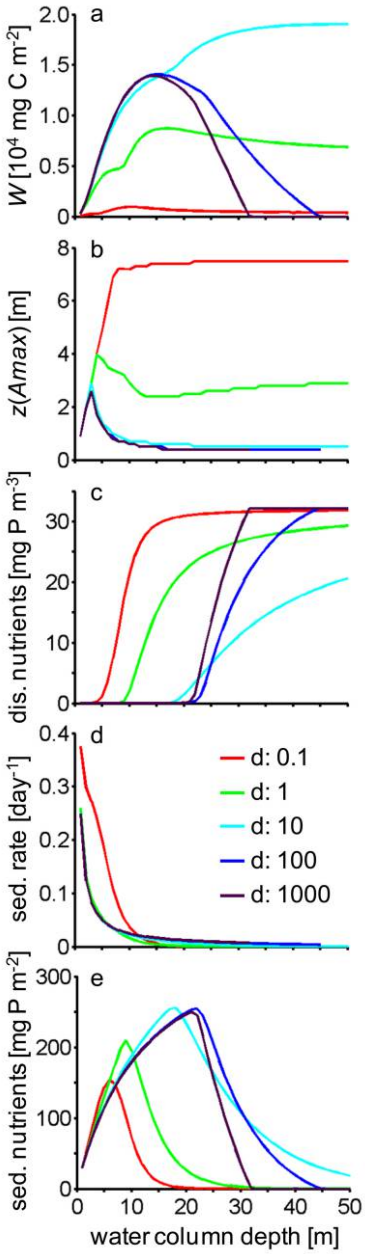

Figure 2: Standard model. Effects of water column depth and mixing intensity (indicated by the coefficient of turbulent diffusion d) on equilibrium values of (*a*) the standing stock of algal biomass integrated over the water column, (*b*) the depth at which the vertical algal biomass profile has its maximum, (*c*) the depth-averaged concentration of dissolved nutrients, (*d*) the algal sedimentation rate, and (*e*) the pool of nutrients in the sediment layer. Algae die out at total water column depths >45 and >32 m at $d = 100$ and $d = 1000$ m^2 day^{-1}, respectively. Accordingly, $z(A_{max})$ and sedimentation rate are not shown for these water column depths.

water column depth, but it starts to decline at intermediate water column depths (figs. 1*q*, 1*v*, 2*a*), when algae become entrained into increasingly deeper aphotic layers (fig. 1*t*, 1*y*, *dark blue*). With further increases in water column depth, the aphotic portion of the water column increases until eventually the water column exceeds a critical depth where depth-integrated light supply is too low to sustain an algal population (Huisman et al. 1999). This critical depth is somewhat smaller at higher turbulence, where algal entrainment to aphotic depths is strongest (figs. 1*q*, 1*t*, 1*v*, 1*y*, 2*a*).

At the other extreme, low turbulence ($d = 0.1$–1 m^2 day^{-1}) promotes the establishment of pronounced vertical gradients. Slow transport of dissolved nutrients from a depth to the surface and weak algal entrainment produce a steep vertical gradient in the algal C : P ratio (fig. 1*d*, 1*i*). Consequently, specific algal production is strongly nutrient limited at the water surface. At the lowest turbulence ($d = 0.1$), specific production therefore peaks several meters below the surface (fig. 1*e*), where nutrient limitation is less severe (i.e., algal C : P is lower) and light availability is still moderate. At somewhat higher turbulence ($d = 1$), nutrients are slightly less limiting at the surface (fig. 1*i*) and stronger self-shading (fig. 1*g*) makes light more limiting at depth, producing a more even distribution of specific production across the upper 3–5 m (fig. 1*j*). Algal sinking is only weakly counteracted by turbulent mixing. Algal biomass therefore has its maximum below the depth of maximal specific production (fig. 1*b*, 1*g*) and is rather low overall (fig. 2*a*), as most nutrients are locked up in the sediment (shallow water columns; figs. 1*a*, 1*f*, 2*e*) or at aphotic depths (deep water columns; figs. 1*c*, 1*h*, 2*c*). In very shallow water columns, algal biomass has a maximum closest to the site of nutrient regeneration, that is, just above the sediment surface (fig. 1*b*, 1*g*). When the water column becomes so deep as to be aphotic at the bottom (7.5 m at $d = 0.1$, 4.5 m at $d = 1$), the biomass maximum detaches from the sediment surface (figs. 1*b*, 1*g*, 2*b*). In sufficiently deep water columns, sinking biomass and particulate nutrients never reach the sediment and are instead respired and released into the water column while algae sink through the aphotic zone. Dissolved nutrients therefore accumulate in the aphotic zone (fig. 1*c*, 1*h*), whereas algal sedimentation rate and nutrients in the sediment approach 0 (fig. 2*d*, 2*e*). Consequently, mineralization of sediments becomes negligible as a limiting step in the regeneration of nutrients, resulting in a step-like biomass increase at the water column depth where the stock of sedimented nutrients starts to decline (fig. 2*a*, 2*e*). With further increasing water column depth, the steepness of the nutrient gradient in the aphotic layer decreases somewhat (fig. 1*c*, 1*h*), reducing the speed of upward transport of dissolved nutrients and, consequently, reducing

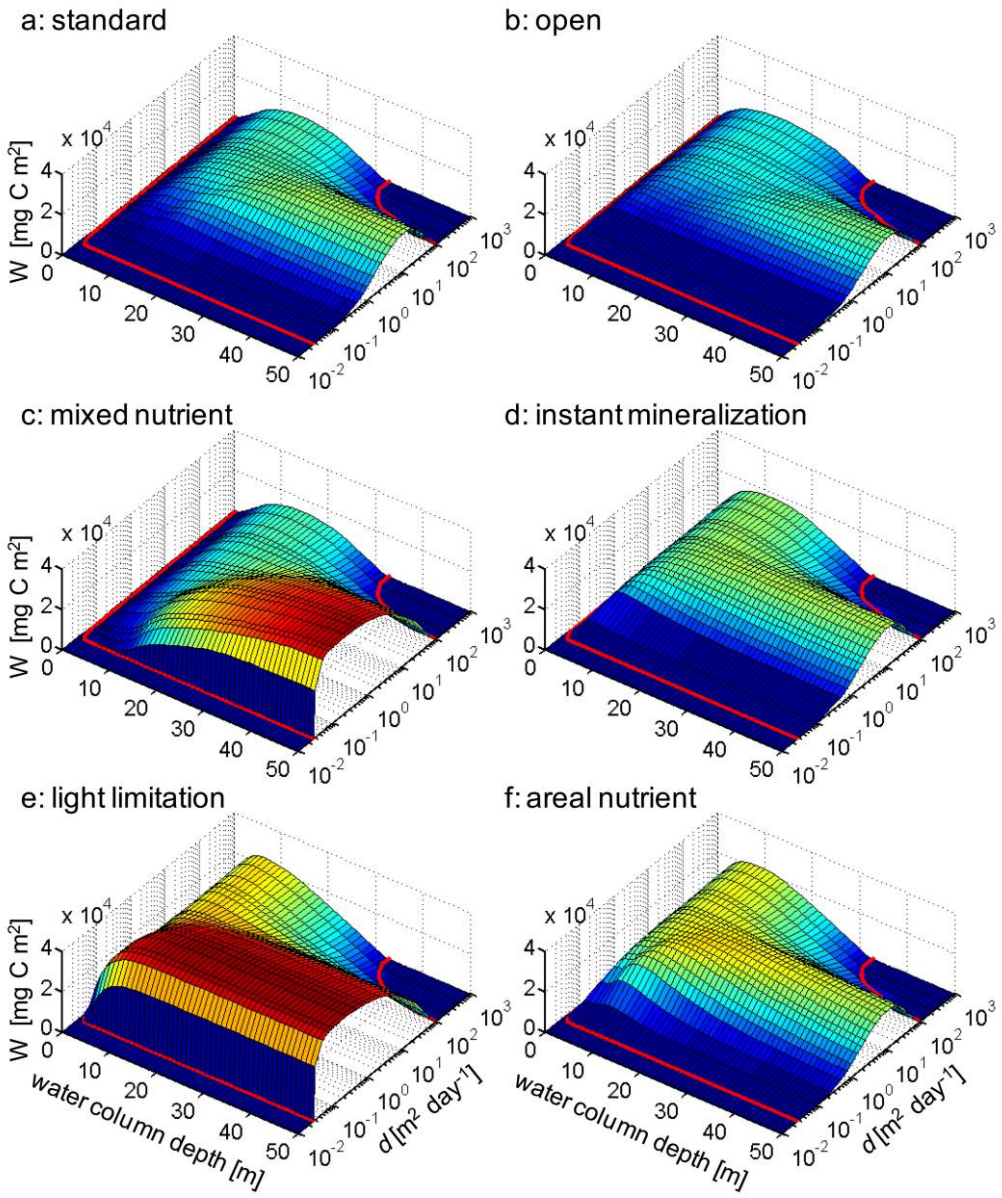

Figure 3: Effects of water column depth and mixing intensity on the standing stock of algal biomass integrated over the water column in (*a*) the standard model, (*b*) the open model, (*c*) the mixed-nutrient model, (*d*) the instant-mineralization model, (*e*) the light-limitation model, and (*f*) the areal-nutrient model. Red lines indicate persistence boundaries.

total biomass (fig. 2*a*). Eventually, depth profiles become independent of water column depth (fig. 1*b*–1*e*, 1*g*–1*j*), and depth-integrated biomass approaches an asymptote (fig. 2*a*). At $d = 0.1$, the asymptotic attractor is a limit cycle with a very small amplitude (fig. 1*d*, 1*e*; see further treatment in "Discussion"). Overall, depth-integrated biomass is, in shallow water columns, most strongly limited by the rates of algal sinking and mineralization in the sediment, and in deep water columns it is limited by the turbulent upward transport of nutrients; therefore, it peaks at intermediate water column depths (fig. 2*a*).

The most complex patterns arise at intermediate turbulence ($d = 10$ m^2 day^{-1}), where the system is nearly well mixed in shallow water columns but exhibits distinct vertical gradients in deep water columns. Until a water column depth of ~15 m, vertical profiles and depth-

integrated/depth-averaged values of all variables are therefore very similar to the well-mixed cases ($d \geq 100$ m^2 day^{-1}; figs. 1, 2). In deeper water columns, a turbulence of $d = 10$ m^2 day^{-1} is not sufficient to mix down a major part of the algal population below the euphotic zone (fig. 1*l*), but nutrient transport to the surface is still fast enough to yield low algal C : P ratios and sustain an algal production maximum at the surface (fig. 1*n*, 1*o*). Consequently, intermediate turbulence yields by far the highest depth-integrated biomass in deep water columns (fig. 2*a*), where production is limited by entrainment to aphotic depths in more strongly mixed systems and by slow upward transport of nutrients in more weakly mixed systems.

Robustness of the Observed Patterns

Extensive numerical runs confirm that the above-described patterns are robust against parameter changes. This is illustrated with a few examples in which total nutrient content, background turbidity, and algal sinking velocity were varied over ecologically relevant ranges (initial $R_d = 10$ vs. 30 mg P m^{-3}; $k_{bg} = 0.2$–0.8 m^{-1}; $v = 0$–0.5 m day^{-1}). These parameters affect the absolute values of most state variables in obvious ways (e.g., lower algal biomass at lower total nutrient content, higher background turbidity, and higher sinking velocity). Clearly, however, at a given total nutrient content, background turbidity, or sinking velocity, changes in water column depth and turbulence consistently produce the same qualitative patterns as described above (fig. A1). Most notably, the highest depth-integrated biomasses are always attained at high water column depths and intermediate levels of turbulence.

Numerical runs also show that the qualitative effects of water column depth and turbulence on the system do not depend on the assumption of flexible algal nutrient stoichiometry. Assuming that algal nutrient stoichiometry is fixed at the Redfield ratio has only relatively minor quantitative effects on most state variables; in contrast, the qualitative patterns produced by changes in water column depth and turbulence are remarkably similar between the fixed-stoichiometry and the standard (flexible-stoichiometry) models (cf. fig. 2 with fig. A2).

Finally, the results are also robust against the relaxation of the assumption of a direct contact of the water column with the sediment. In fact, when the exchange rate between surface and deep water layers is set to a value typical of a sharp thermocline ($a = 0.1$), the results of the open and standard models are strikingly similar (fig. 3*b* vs. fig. 3*a*).

Light, Nutrients, or Sinking Losses: What Limits Algal Biomass?

There is a striking symmetry in the effects of water column depth and turbulence on phytoplankton net production that is most easily observed from a three-dimensional plot of depth-integrated algal biomass in *z*-*d* space (fig. 3*a*, 3*b*). On the one hand, low mixing intensity has a twofold negative effect on algal net growth, which is independent of water column depth: first, sinking of algae out of the photic zone is hardly counteracted; second, the upward transport of nutrients to photic depths is very slow. On the other hand, low water column depth also has a twofold negative effect on algal net growth, which, in turn, is independent of turbulence: first, high sinking rates in shallow water columns impose high direct losses on the population, and second, they deplete the water column of nutrients. Finally, the combination of high mixing intensity and a deep water column causes downmixing of phytoplankton to aphotic depths and, consequently, results in severe light limitation of algal production. Thus, depending on the exact combination of water column depth and mixing intensity, depth-integrated algal biomass may be limited predominantly by sinking losses, nutrient (re-)supply, or light availability. As a result, depth-integrated biomass forms an approximately rectangular ridge in *z*-*d* space, with the highest biomasses occurring at intermediate water column depths and/or intermediate levels of turbulence (fig. 3*a*, 3*b*).

We explored in detail the mechanisms limiting algal biomass by comparing the standard model with the mixed-nutrient, instant-mineralization, areal-nutrient, and light-limitation models. These analyses reveal that limitation by light and sinking losses set the persistence boundaries of the phytoplankton population in *z*-*d* space, whereas nutrient (re-)supply limits algal biomass inside the persistence region (fig. 3). The factors limiting phytoplankton persistence and biomass are discussed below.

The persistence boundaries are essentially identical in all model variants (fig. 3). That this must be the case can be observed in an invasion analysis. In an empty system, algal biomass, particulate nutrients, and sedimented nutrients are all initially 0. Consequently, all nutrients are present in mineral form, allowing fast nutrient uptake by invading algae. Unless the overall nutrient content of the system and/or the algal nutrient uptake rate is extremely low, the nutrient quota of invading algae is therefore maximal and algal growth is purely light limited in the standard, instant-mineralization, areal-nutrient, and mixed-nutrient models as well. Conditions that are sufficient for successful invasion by a purely light-limited population are then also sufficient for successful invasion by a potentially nutrient-limited population. Persistence is therefore fully explained by existing theory of light-limited sys-

tems, for which Huisman and Sommeijer (2002) have identified four persistence boundaries: (1) a minimal turbulence (at $d = 0.03\ m^2\ day^{-1}$ in fig. 3) where entrainment and growth cannot counteract sinking losses, (2) a minimal depth (at $z = 0.4$ m in fig. 3) where algal growth cannot compensate for sinking losses, and the combination of (3) a critical turbulence and (4) a critical depth (at $d = 77\ m^2\ day^{-1}$ and $z = 32$ m in fig. 3) where algae cannot outgrow downmixing to aphotic depths.

All other parameters being equal, for a given combination of water column depth and turbulence within the persistence boundaries, the light-limited system attains the highest algal biomass, the standard system always attains the lowest algal biomass, and the mixed-nutrient, instant-mineralization, and areal-nutrient models take intermediate positions (fig. 3). A comparison of the five models supports the following interpretations of the mechanisms limiting biomass in the standard model: (1) In deep water columns with intermediate to low turbulence, algal biomass is highest in the light-limitation and mixed-nutrient models, suggesting that algal biomass in the standard model is limited by the turbulent-transport rate of mineralized nutrients from aphotic depths. (2) In turbulent water columns of shallow to intermediate depth, algal biomass is highest in the light-limitation and areal-nutrient models, intermediate in the instant-mineralization model, and lowest in the mixed-nutrient and standard models, suggesting that algal biomass in the latter two models is limited by the total (areal) amount of nutrients in the system and the mineralization rate of nutrients in the sediment. (3) In shallow water columns with low turbulence, algal biomass is highest in the light-limitation model and lower in all other models, suggesting that algal biomass in the standard model is limited by a combination of slow mineralization in the sediment and slow upward transport of mineralized nutrients. (4) Near the upper persistence boundaries in *z*-*d* space, all models attain similar biomasses, which suggests that algal biomass is light limited in deep, turbulent water columns.

The contrasting influences of water column depth and turbulence on nutrient versus light limitation are also reflected in the position and shape of the optimal turbulence isoline, that is, the turbulence yielding the highest (areal) biomass at a given water column depth (fig. 4). In the standard model, increased light limitation (e.g., increasing background turbidity) moves optimal turbulence toward lower mixing intensities, where downmixing of phytoplankton to light-limited layers is reduced; in contrast, increased nutrient limitation (e.g., decreasing total nutrients in the system) moves optimal turbulence toward higher mixing intensities, where upward transport of nutrients is increased (fig. 4*a*). For the same reasons, optimal turbulence is lowest in the light-limitation model and highest in the standard model, and the mixed-nutrient model is intermediate (fig. 4*b*).

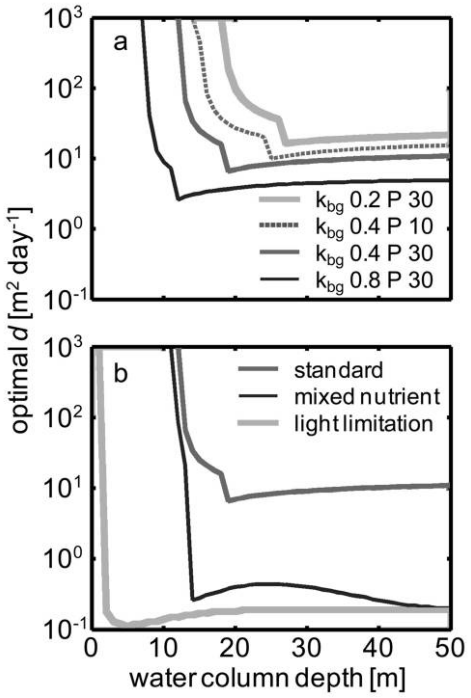

Figure 4: *a*, Effects of water column depth on optimal mixing intensity (mixing intensity yielding the highest depth-integrated biomass for a given water column depth) in the standard model at different background turbidities (k_{bg}, m^{-1}) and initial nutrient concentrations (P, mg P m^{-3}), as indicated. *b*, Effects of water column depth on optimal mixing intensity in the standard, mixed-nutrient, and light-limitation models.

Discussion

We have asked in a very general way how water column depth and turbulence affect the vertical distributions of phytoplankton and dissolved, suspended, and sedimented nutrients and how physical constraints on the vertical fluxes of light, nutrients, and algae limit the biomass of pelagic primary producers. Our theoretical analysis reveals that sinking losses and light supply determine the persistence boundaries of a population of sinking algae in *z*-*d* space. This merely confirms the results Huisman and Sommeijer (2002) obtained for light-limited phytoplankton, but it is important to realize that these results extend to potentially nutrient-limited phytoplankton. Most natural phytoplankton populations are, indeed, at least colimited by nutrients. In the absence of lateral nutrient fluxes and within the persistence boundaries set by sinking losses and light supply, phytoplankton biomass is then expected to

be most strongly limited by the processes determining nutrient supply to the photic zone.

Our analysis suggests that nutrient availability in shallow water columns is most strongly limited by the mineralization rate in the sediment (or by the influx across a sharp thermocline), whereas in deep water columns, turbulent upward transport of mineralized nutrients is most limiting. The highest depth-integrated production is therefore sustained in deep water columns with intermediate turbulence, where algal sinking losses to the sediment are very low (because algal biomass is respired and mineralized before it reaches the bottom) and the turbulent upward transport of nutrients mineralized in the aphotic strata is relatively fast. In other words, phytoplankton production and biomass are higher the higher the net vertical transport rate of nutrients from the nutrient regeneration zone (sediment and/or deep water) to the nutrient use zone by primary producers (well-lit surface strata). This parallels a similar result obtained by Cloern (2007), who analyzed the influence of lateral connectivity between a shallow, well-lit but nutrient-depleted habitat and a deep, light-limited but nutrient-replete habitat and found that overall productivity (averaged across both habitats) was higher the higher the water-exchange rate and, thus, the higher the nutrient transport rate from the deep to the shallow habitats.

Transient Dynamics, Persistent Oscillations, and Competitive Interactions

Differences in the speed of the two major, opposite vertical nutrient fluxes (sinking of particulate nutrients and upward flux of recycled, dissolved nutrients) are responsible not only for steady-state biomass patterns in *z*-*d* space but also for the development of transient phytoplankton blooms under most environmental conditions. From initial conditions of high dissolved-nutrient concentration, an algal population starting from low initial density always goes through a transient bloom (usually after 10–50 days) before settling on its asymptotic trajectory, with the exception of those populations exposed to strongly light-limited conditions that are close to the persistence boundary at high water column depths and high turbulence (C. Jäger, unpublished results). This happens because the initially high dissolved-nutrient concentration stimulates fast algal growth in the upper, well-lit layers that is followed by algal sinking and rapid nutrient depletion, which terminates the bloom (see Huppert et al. 2002). Algal sinking leads to a relatively fast downward flux of particulate nutrients. The latter is only slowly counteracted by turbulent upward transport of recycled nutrients from aphotic depths, which subsequently sustains a steady-state biomass that is much smaller than the transient peak biomass.

The interaction of these opposed vertical nutrient fluxes can actually generate persistent oscillations or even chaotic population dynamics of algal biomass. Such attractors occur if, after an algal bloom, nutrients are completely depleted in the euphotic zone and when the timescale of algal downward flux is fast compared with the timescale of the nutrient upward flux (Huisman et al. 2006). Usually these requirements are met at low mixing intensities and high algal sinking velocities. The timescale of the nutrient upward flux increases with decreasing mixing intensity and increasing water column depth. Hence, in our model, persistent oscillations occur at the lowest mixing intensity ($d = 0.1$ m^2 day^{-1}) and in deep water columns. The oscillations become more pronounced at a lower overall nutrient content of the system (initial $R_d = 10$ μg P L^{-1}), where the nutrient upward flux is reduced, and at a higher light supply ($k_{bg} = 0.2$ m^{-1}), where production is possible at greater depths and, consequently, net mineralization in the water column is reduced and more nutrients are mineralized in the sediment layer (fig. A1).

In real plankton communities consisting of multiple species, the dynamic interplay of algal sinking and nutrient recycling at aphotic depths will affect the outcome of competitive interactions among phytoplankton taxa differing in their buoyancy regulation capabilities. For example, in the absence of nutrient limitation, buoyant taxa will often have a competitive advantage under conditions of low turbulence through the formation of surface blooms, thus shading the deep water layers where sinking taxa tend to accumulate (Visser et al. 1996; Huisman et al. 2004). Surface blooms, however, can be sustained only when enough nutrients are supplied to the upper water layers to support algal growth (Yoshiyama et al. 2009). In field enclosures with low turbulent mixing, Jäger et al. (2008*a*) observed that an initial dominance of motile species occupying the upper strata of the water column was replaced by a dominance of fast-sinking diatoms when nutrients became limited at the surface. A plausible explanation for this phenomenon (consistent with observed vertical profiles of dissolved nutrients) is that the diatoms, which primarily occupy the deeper strata of the water column, intercepted the upward transport of recycled nutrients, causing severe nutrient limitation at the surface.

Spatial Structure, Flexible Algal Stoichiometry, and Higher Trophic Levels

In the simple two-compartment model of Cloern (2007), the beneficial effects on algal production of a high (lateral) exchange rate between a shallow, nutrient-limited habitat and a deep, light-limited habitat are directly transmitted to the next-higher trophic level; that is, the production of herbivorous zooplankton (averaged across both habitats)

is higher the higher the (passive) exchange rate of nutrients and organisms between the two habitats. In contrast, in our model, increased primary production may not always translate into increased herbivore production for at least two reasons. First, in contrast to Cloern (2007), we assumed that algal carbon-to-nutrient stoichiometry is flexible. Second, the distance between nutrient- and light-limited habitats is short enough to be easily covered by (vertically) migrating herbivores, potentially decoupling the transport rates of nutrients, algae, and herbivores.

Our model analyses suggest that the qualitative influences of water column depth and turbulence on a phytoplankton system lacking herbivores are not crucially dependent on the assumption of flexible versus fixed algal carbon-to-nutrient stoichiometry. In a system with herbivores, flexible producer stoichiometry may, however, lead to a mismatch of producer elemental composition and herbivore nutrient requirements. In particular, depending on the light-to-nutrient supply ratio, there is often a trade-off between food quantity (algal carbon density) and food quality (carbon-to-nutrient ratio of algal biomass; Urabe and Sterner 1996). In water columns of differing depths and turbulence, herbivore production may therefore not always follow the same pattern as primary production. For well-mixed water columns, an extension of our model that included herbivores indeed suggests that low algal quality (high algal C : P ratio) can limit herbivore biomass at relatively shallow depths (more generally speaking, at a relatively high light supply) where algal biomass in the absence of grazers would be close to maximal (Diehl 2007; Jäger et al. 2008*b*), a phenomenon called the paradox of energy enrichment that has been observed in several experiments (Andersen et al. 2004).

In incompletely mixed water columns, the situation is more complex. Mobile grazers such as *Daphnia* can sense vertical gradients in foraging profitability (determined by algal density and quality) and move along them toward the depth that offers optimal food conditions (Schatz and McCauley 2007). Additionally, grazers performing diel vertical migrations could benefit from carbon-rich algal food close to the surface during the night and nutrient-rich food in deeper layers during the day (Sterner and Schwalbach 2001). Because grazers rarely incorporate all ingested nutrients into new biomass, vertically migrating herbivores may furthermore act as a vector moving particulate nutrients from the ingestion depth to the waste excretion depth. In particular, at very low mixing intensities, this additional nutrient transport may alleviate the severe nutrient limitation observed in well-lit upper strata in the absence of grazers. Thus, many more processes may contribute to the vertical transport of grazers, algae, and nutrients in weakly mixed versus well-mixed water columns. Preliminary modeling suggests that grazer biomass indeed responds differently to water column depth in stratified versus well-mixed water columns (S. Diehl, unpublished results).

Physical Water Column Structure and Community Dynamics

Ecologists increasingly appreciate the roles of spatial structure and biological and physical transport processes as mechanisms of population, community, and ecosystem dynamics (Polis et al. 1997; Reiners and Driese 2001). Physical factors like the depth of a surface layer and the intensity of its mixing are major determinants of spatial habitat structure and vertical transport processes in pelagic systems. Driven by weather and climate, these physical factors can be highly variable. In the actual debate on global climate change, the physical environment has therefore been set into new focus (Behrenfeld et al. 2006; Falkowski and Oliver 2007). For example, there is evidence that global warming will lead to earlier and more shallow stratification and increased water column stability (Sarmiento et al. 1998; Lehman 2000; Coats et al. 2006; George and Hewitt 2006). In temperate lakes, the timing and depth of stratification, in turn, set the stage for events such as the phytoplankton spring bloom, a clearwater phase caused by intense grazing, and the subsequent establishment of a summer community (Sommer et al. 1986; Straile 2002; Berger et al. 2006, 2007; Peeters et al. 2007). Clearly, the physical structure of the water column has potentially far-reaching implications not only for ecosystem processes (primary production, sinking export, nutrient recycling, etc.) but also for community processes such as food web dynamics and seasonal succession. We have recently shown that equilibrium conditions of a simple, well-mixed algae-nutrient system yield important insights into the behavior of a trophically more complex system (Jäger et al. 2008*b*). We therefore believe that a fundamental understanding of the effects of environmental change on multitrophic, pelagic systems will greatly benefit from the very general insights provided by our study into the impacts of water column depth and turbulence on processes at the autotrophic food web base.

Acknowledgments

We thank O. Richter for the introduction to COMSOL and F. Haupt for help with the numerical simulations. We also thank M. A. Evans, C. Klausmeier, E. Litchman, J. Mellard, K. Yoshiyama, and two anonymous reviewers for their helpful comments. This study was supported by funding from Deutsche Forschungsgemeinschaft (DI 745/2–4).

Literature Cited

Andersen, T. 1997. Pelagic nutrient cycles: herbivores as sources and sinks. Springer, New York.

Andersen, T., J. J. Elser, and D. O. Hessen. 2004. Stoichiometry and population dynamics. Ecology Letters 7:884–900.

Antia, A. N. 2005. Solubilization of particles in sediment traps: revising the stoichiometry of mixed layer export. Biogeosciences 2: 189–204.

Behrenfeld, M. J., R. T. O'Malley, D. A. Siegel, C. R. McClain, J. L. Sarmiento, G. C. Feldman, A. J. Milligan, P. G. Falkowski, R. M. Letelier, and E. S. Boss. 2006. Climate-driven trends in contemporary ocean productivity. Nature 444:752–755.

Berger, S. A., S. Diehl, T. J. Kunz, D. Albrecht, A. M. Oucible, and S. Ritzer. 2006. Light supply, plankton biomass, and seston stoichiometry in a gradient of lake mixing depths. Limnology and Oceanography 51:1898–1905.

Berger, S. A., S. Diehl, H. Stibor, G. Trommer, M. Ruhenstroth, A. Wild, A. Weigert, C. G. Jäger, and M. Striebel. 2007. Water temperature and mixing depth affect timing and magnitude of events during spring succession of the plankton. Oecologia (Berlin) 150: 643–654.

Bertilsson, S., O. Berglund, D. M. Karl, and S. W. Chisholm. 2003. Elemental composition of marine *Prochlorococcus* and *Synechococcus*: implications for the ecological stoichiometry of the sea. Limnology and Oceanography 48:1721–1731.

Christian, J. R. 2005. Biogeochemical cycling in the oligotrophic ocean: Redfield and non-Redfield models. Limnology and Oceanography 50:646–657.

Cloern, J. E. 2007. Habitat connectivity and ecosystem productivity: implications from a simple model. American Naturalist 169:E21–E33.

Coats, R., J. Perez-Losada, G. Schladow, R. Richards, and C. Goldman. 2006. The warming of Lake Tahoe. Climatic Change 76:121–148.

Condie, S. A., and M. Bormans. 1997. The influence of density stratification on particle settling, dispersion and population growth. Journal of Theoretical Biology 187:65–75.

Diehl, S. 2002. Phytoplankton, light, and nutrients in a gradient of mixing depths: theory. Ecology 83:386–398.

———. 2007. Paradoxes of enrichment: effects of increased light versus nutrient supply on pelagic producer-grazer systems. American Naturalist 169:E173–E191.

Diehl, S., S. Berger, R. Ptacnik, and A. Wild. 2002. Phytoplankton, light, and nutrients in a gradient of mixing depths: field experiments. Ecology 83:399–411.

Diehl, S., S. Berger, and R. Wöhrl. 2005. Flexible nutrient stoichiometry mediates environmental influences, on phytoplankton and its resources. Ecology 86:2931–2945.

Elser, J. J., and N. B. George. 1993. The stoichiometry of N and P in the pelagic zone of Castle Lake, California. Journal of Plankton Research 15:977–992.

Falkowski, P. G., and M. J. Oliver. 2007. Mix and match: how climate selects phytoplankton. Nature Reviews Microbiology 5:813–819.

Geider, R. J., H. L. MacIntyre, and T. M. Kana. 1998. A dynamic regulatory model of phytoplanktonic acclimation to light, nutrients, and temperature. Limnology and Oceanography 43:679–694.

George, D. C., and D. P. Hewitt. 2006. The impact of year-to-year changes in the weather on the dynamics of *Daphnia* in a thermally stratified lake. Aquatic Ecology 40:33–47.

Huisman, J. 1999. Population dynamics of light-limited phytoplankton: microcosm experiments. Ecology 80:202–210.

Huisman, J., and B. Sommeijer. 2002. Maximal sustainable sinking velocity of phytoplankton. Marine Ecology Progress Series 244:39–48.

Huisman, J., and F. J. Weissing. 1995. Competition for nutrients and light in a mixed water column: a theoretical analysis. American Naturalist 146:536–564.

Huisman, J., P. van Oostveen, and F. J. Weissing. 1999. Critical depth and critical turbulence: two different mechanisms for the development of phytoplankton blooms. Limnology and Oceanography 44:1781–1787.

Huisman, J., M. Arrayas, U. Ebert, and B. Sommeijer. 2002. How do sinking phytoplankton species manage to persist? American Naturalist 159:245–254.

Huisman, J., J. Sharples, J. M. Stroom, P. M. Visser, W. E. A. Kardinaal, J. M. H. Verspagen, and B. Sommeijer. 2004. Changes in turbulent mixing shift competition for light between phytoplankton species. Ecology 85:2960–2970.

Huisman, J., N. N. P. Thi, D. M. Karl, and B. Sommeijer. 2006. Reduced mixing generates oscillations and chaos in the oceanic deep chlorophyll maximum. Nature 439:322–325.

Huppert, A., B. Blasius, and L. Stone. 2002. A model of phytoplankton blooms. American Naturalist 159:156–171.

Jäger, C. G., S. Diehl, and G. M. Schmidt. 2008*a*. Influence of water-column depth and mixing on phytoplankton biomass, community composition, and nutrients. Limnology and Oceanography 53: 2361–2373.

Jäger, C. G., S. Diehl, C. Matauschek, C. A. Klausmeier, and H. Stibor. 2008*b*. Transient dynamics of pelagic producer-grazer systems in a gradient of nutrients and mixing depths. Ecology 89:1272–1286.

Kirk, J. T. O. 1994. Light and photosynthesis in aquatic ecosystems. 2nd ed. Cambridge University Press, Cambridge.

Klausmeier, C. A., and E. Litchman. 2001. Algal games: the vertical distribution of phytoplankton in poorly mixed water columns. Limnology and Oceanography 46:1998–2007.

Lehman, P. W. 2000. The influence of climate on phytoplankton community biomass in San Francisco Bay Estuary. Limnology and Oceanography 45:580–590.

O'Brien, K. R., G. N. Ivey, D. P. Hamilton, A. M. Waite, and P. M. Visser. 2003. Simple mixing criteria for the growth of negatively buoyant phytoplankton. Limnology and Oceanography 48:1326–1337.

Park, S., S. Chandra, D. C. Müller-Navarra, and C. R. Goldman. 2004. Diel and vertical variability of seston food quality and quantity in a small subalpine oligomesotrophic lake. Journal of Plankton Research 26:1489–1498.

Peeters, F., D. Straile, A. Lorke, and D. Ollinger. 2007. Turbulent mixing and phytoplankton spring bloom development in a deep lake. Limnology and Oceanography 52:286–298.

Peterson, M. L., S. G. Wakeham, C. Lee, M. A. Askea, and J. C. Miquel. 2005. Novel techniques for collection of sinking particles in the ocean and determining their settling rates. Limnology and Oceanography Methods 3:520–532.

Polis, G. A., W. B. Anderson, and R. D. Holt. 1997. Toward an integration of landscape and food web ecology: the dynamics of spatially subsidized food webs. Annual Review of Ecology and Systematics 28:289–316.

Ptacnik, R., S. Diehl, and S. Berger. 2003. Performance of sinking

and nonsinking phytoplankton taxa in a gradient of mixing depths. Limnology and Oceanography 48:1903–1912.

Reiners, W. A., and K. L. Driese. 2001. The propagation of ecological influences through heterogeneous environmental space. BioScience 51:939–950.

Reynolds, C. S. 1984. The ecology of freshwater phytoplankton. Cambridge University Press, Cambridge.

Riley, G. A., H. Stommel, and D. F. Bumpus. 1949. Quantitative ecology of the plankton of the western North Atlantic. Bulletin of the Bingham Oceanographic Collection of Yale University 12:1–169.

Rothhaupt, K. O. 1991. Variations on the zooplankton menu: reply. Limnology and Oceanography 36:824–827.

Sarmiento, J. L., T. M. C. Hughes, R. J. Stouffer, and S. Manabe. 1998. Simulated response of the ocean carbon cycle to anthropogenic climate warming. Nature 393:245–249.

Schatz, G. S., and E. McCauley. 2007. Foraging behavior by *Daphnia* in stoichiometric gradients of food quality. Oecologia (Berlin) 153: 1021–1030.

Senft, H. 1978. Dependence of light-saturated rates of algal photosynthesis on intracellular concentrations of phosphorus. Limnology and Oceanography 23:709–718.

Smayda, T. J. 1969. Some measurements of sinking rate of fecal pellets. Limnology and Oceanography 14:621–625.

Sommer, U., Z. M. Gliwicz, W. Lampert, and A. Duncan. 1986. The peg-model of seasonal succession of planktonic events in fresh waters. Archiv für Hydrobiologie 106:433–471.

Sterner, R. W., and M. S. Schwalbach. 2001. Diel integration of food quality by *Daphnia*: luxury consumption by a freshwater planktonic herbivore. Limnology and Oceanography 46:410–416.

Sterner, R. W., J. J. Elser, E. J. Fee, S. J. Guildford, and T. H. Chrzanowski. 1997. The light : nutrient ratio in lakes: the balance of energy and materials affects ecosystem structure and process. American Naturalist 150:663–684.

Straile, D. 2002. North Atlantic Oscillation synchronizes food-web interactions in central European lakes. Proceedings of the Royal Society B: Biological Sciences 269:391–395.

Sverdrup, H. U. 1953. On conditions for the vernal blooming of phytoplankton. Journal du Conseil: Conseil Permanent International pour l'Exploration de la Mer 18:287–295.

Urabe, J., and R. W. Sterner. 1996. Regulation of herbivore growth by the balance of light and nutrients. Proceedings of the National Academy of Sciences of the USA 93:8465–8469.

Visser, P. M., L. Massaut, J. Huisman, and L. R. Mur. 1996. Sedimentation losses of *Scenedesmus* in relation to mixing depth. Archiv fur Hydrobiologie 136:289–308.

Wetzel, R. G. 1983. Limnology. 2nd ed. Saunders, Philadelphia.

Yoshiyama, K., J. P. Mellard, E. Litchman, and C. A. Klausmeier. 2009. Phytoplankton competition for nutrients and light in a stratified water column. American Naturalist 174:190–203.

Associate Editor: Franz J. Weissing
Editor: Donald L. DeAngelis